European Journal of Neuroscience, Vol. 26, pp. 890–902, 2007 doi:10.1111/j.1460-9568.2007.05697.x

Co-localization and functional cross-talk between A_1 and $P2Y_1$ purine receptors in rat hippocampus

I. Tonazzini,[1] M. L. Trincavelli,[1] J. Storm-Mathisen,[2] C. Martini[1] and L. H. Bergersen[2]
[1]Department of Psychiatry Neurobiology Pharmacology and Biotechnology, University of Pisa, via Bonanno 6, 56126, Pisa, Italy
[2]Department of Anatomy, IMB, and Centre for Molecular Biology and Neuroscience (CMBN), University of Oslo, PO Box 1105, Blindern, NO-0317, Oslo, Norway

Keywords: adenosine, ATP, brain damage, electron microscopy, G protein coupled receptors, immunocytochemistry

OnlineOpen: This article is available free online at www.blackwell-synergy.com

Abstract

Adenosine and ATP, via their specific P1 and P2 receptors, modulate a wide variety of cellular and tissue functions, playing a neuroprotective or neurodegenerative role in brain damage conditions. Although, in general, adenosine inhibits excitability and ATP functions as an excitatory transmitter in the central nervous system, recent data suggest the existence of a heterodimerization and a functional interaction between P1 and P2 receptors in the brain. In particular, interactions of adenosine A_1 and $P2Y_1$ receptors may play important roles in the purinergic signalling cascade. In the present work, we investigated the subcellular localization/co-localization of the receptors and their functional cross-talk at the membrane level in Wistar rat hippocampus. This is a particularly vulnerable brain area, which is sensitive to adenosine- and ATP-mediated control of glutamatergic transmission. The postembedding immunogold electron microscopy technique showed that the two receptors are co-localized at the synaptic membranes and surrounding astroglial membranes of glutamatergic synapses. To investigate the functional cross-talk between the two types of purinergic receptors, we evaluated the reciprocal effects of their activation on their G protein coupling. $P2Y_1$ receptor stimulation impaired the potency of A_1 receptor coupling to G protein, whereas the stimulation of A_1 receptors increased the functional responsiveness of $P2Y_1$ receptors. The results demonstrated an A_1–$P2Y_1$ receptor co-localization at glutamatergic synapses and surrounding astrocytes and a functional interaction between these receptors in hippocampus, suggesting ATP and adenosine can interact in purine-mediated signalling. This may be particularly important during pathological conditions, when large amounts of these mediators are released.

Introduction

ATP and adenosine, via their specific P2 and P1 purinergic receptors (Fredholm *et al*., 1994), mediate a wide variety of physiological processes including neuromodulation and neurotransmission. Moreover, the purinergic system has been implicated in many pathological and neurodegenerative conditions, in which massive release of ATP and, in turn, ADP and adenosine production, occur from damaged or dying cells, i.e. following ischemia, necrosis or trauma (Rathbone *et al*., 1999; Burnstock, 2004). Several reports have described a dualistic neuroprotective-neuromodulatory role of ATP interacting with the specific ionotropic receptors (P2XR) and G protein coupled receptors (GPCRs; P2YR) (Fredholm *et al*., 1994). Among P2YR, $P2Y_1$ receptors ($P2Y_1R$) appear to be of particular interest in pathophysiological mechanisms with both detrimental and beneficial effects (Franke & Illes, 2006). On the other hand, through the activation of the inhibitory A_1 adenosine receptor (A_1R) coupled to G proteins (Dunwiddie & Masino, 2001), adenosine inhibits the release of excitatory neurotransmitters and decreases neuronal excitability, exerting a neuroprotective role (Wardas, 2002).

Recent data have provided evidence for the existence of an association between A_1R and $P2Y_1R$. In a co-transfected cell line model these receptors interact directly (Yoshioka & Nakata, 2004) to generate a hetero-oligomer, which has novel pharmacological and functional characteristics indicating a potential role in the purinergic-signalling cascade. A_1R and $P2Y_1R$ have been suggested to be involved in the modulation of brain damage and contribute, alone or in combination, to neuro-degenerative/-regenerative processes (Neary *et al*., 2003; Franke & Illes, 2006; Von Kugelgen, 2006). Moreover, co-localization of these receptors has been demonstrated by immunofluorescence and immunoprecipitation (Yoshioka *et al*., 2002). However, no data are at present available on the precise localization/co-localization of A_1 and $P2Y_1$ receptors at cellular and subcellular levels, or on their reciprocal modulation/functional interaction in the native brain.

Hippocampus is a brain area with a specific vulnerability to injuries, in particular to ischemia (Harry & Lefebvre d'Hellencourt, 2003). In the hippocampus, A_1R and $P2Y_1R$ are particularly abundant (Gottlieb & Matute, 1997; Ochiishi *et al*., 1999; Jimenez *et al*., 2000; Moran-Jimenez & Matute, 2000; Zhu & Kimelberg, 2001) and involved in the modulation of glutamate release (Rudolphi *et al*., 1992; Mendoza-Fernandez *et al*., 2000; Masino *et al*., 2002; Koizumi *et al*., 2003; Kawamura *et al*., 2004; Rodrigues *et al*., 2005; Jourdain *et al*., 2007), hence contributing to neurotransmission and neuro-degenerative and -regenerative processes.

In the present work, we investigated the localization/co-localization of A_1R and $P2Y_1R$ in rat hippocampus, focusing on glutamatergic synapses and using electron microscopic (EM) quantification

Correspondence: Dr Linda H. Bergersen, as above.
E-mail: l.h.bergersen@medisin.uio.no

Received 13 February 2007, revised 30 May 2007, accepted 11 June 2007

of postembedding immunogold labelling; this technique allows the precise localization of proteins to be identified at subcellular resolution, on different parts of astrocytes and neurons.

As a first step to investigate the functional A_1R and $P2Y_1R$ cross-talk, we studied the A_1R activation following $P2Y_1R$ stimulation and vice versa in crude rat hippocampal membranes (HC). For this purpose the [^{35}S]guanosine-5′-(γ-thio)-triphosphate ([^{35}S]GTPγS) binding assay (Lorenzen *et al*., 1993, 1996) was used. The GTP binding represents the initial step of any GPCR activation and of the intracellular signalling cascade mediated by GPCRs (Lorenzen *et al*., 1996).

Materials and methods

Materials

The A_1R antibody was obtained commercially from Alpha Diagnostic International (San Antonio, TX, USA) and the $P2Y_1R$ antibody from Alomone Laboratories (Jerusalem, Israel). The data sheets supplied by the manufacturers showed monospecificity by immunoblotting of rat brain. The A_1R antibody was raised against a 14-amino-acid peptide corresponding to amino acid residues 163–176 of the rat or human receptor protein, i.e. the epitope is in the presumed extracellular N-terminal domain. The $P2Y_1R$ antibody was raised against a 17-amino-acid peptide (C) RALIYKDLDNSPLRRKS, corresponding to residues 242–258 of rat or human $P2Y_1R$, i.e. the epitope location is in the presumed third intracellular loop (i3) between the TM5 and TM6 domains. Secondary antibody, goat anti-rabbit IgG-HRP conjugate, was from Calbiochem (EMD Biosciences, affiliate of Merck kgaA, Darmstadt, Germany). Goat anti-rabbit immunoglobulins coupled to 10-nm or 15-nm gold particles were obtained from Aurion (Wageningen, The Netherlands). Secondary antibody, goat anti-rabbit IgG-HRP conjugate, was from Calbiochem (EMD Biosciences, affiliate of Merck kgaA, Darmstadt, Germany). Electrophoresis reagents were purchased from Bio-Rad (Hercules, CA, USA); full range rainbow molecular weight markers (range 10–250 kDa) were obtained from Amersham Biosciences (Freiburg, Germany).

[^{35}S]GTPγS (specific activity 1000 Ci/mmol) was purchased from Amersham Biosciences Europe GmbH (Freiburg, Germany); adenosine deaminase (ADA) was from Roche Diagnostics GmbH (Mannheim, Germany). N^6-cyclohexyl adenosine (CHA), 8-cyclopentyl-1,3-dipropylxanthine (DPCPX), GDP, guanosine-5′-(γ-thio)triphosphate (GTPγS), 2-methylthio-adenosine 5′-diphosphate (MeSADP), 2′-deoxy-N^6-methyl adenosine 3′,5′-diphosphate (MRS2179), and protease inhibitors were obtained from Sigma Chemical Co (St Louis, MO, USA). The protein concentration of the samples was established using the protein assay based on the Bradford method from Bio-Rad (Hercules, CA, USA), using bovine serum albumin as a standard. All other reagent grade chemicals were supplied from standard commercial sources.

Postembedding immunogold cytochemistry

Immunogold electron microscopy quantification was used to study A_1R and $P2Y_1R$ receptors in rat hippocampus, focusing on glutamatergic synapses. Animals were treated in accordance with the guidelines of the Norwegian Committees on Animal Experimentation (Norwegian Animal Welfare Act and European Communities Council Directive of 24 November 1986-86/609/EEC). Receptor immunocytochemistry was performed as described previously in Bergersen *et al*. (2005), with some modifications. Wistar rats were deeply anesthetized with an i.p. injection of pentobarbital. Briefly, after transcardiac perfusion with 0.1% glutaraldehyde and 4% formaldehyde in 0.1 M sodium phosphate buffer (NaPi), pH 7.4, the brains from adult male Wistar rats (300 g, $n = 3$) were left *in situ* overnight (4 °C). Then hippocampal specimens were isolated, processed by cryoprotection in different glycerol solutions, snap-frozen in liquid propane cooled by liquid nitrogen and embedded in Lowicryl HM 20 through freeze-substitution. Ultrathin sections (80 nm) were cut with a diamond knife on a Reichert-Jung ultramicrotome and mounted on nickel grids (300 mesh square, Electron Microscopy Sciences, USA). The sections were processed at room temperature in solutions of 0.05 M Tris HCl buffer, pH 7.4 containing 0.3% (w/v, for $P2Y_1R$ antibody) or 0.1% (for A_1R antibody) NaCl and 0.1% Triton X-100 (TBST) and completed as stated below.

After 'etching' in sodium ethanolate to remove plastic from tissues, sections were incubated in TBST containing 2% human serum albumin (HSA) for 10 min and then overnight (around 20 h) with specific primary antibodies diluted in TBST containing 2% HSA. Antibodies against A_1R (dilution 2 μg/mL) as well as the antibody against the $P2Y_1R$ (dilution 4 μg/mL) were used. Sections were then incubated with goat anti-rabbit immunoglobulins coupled to 10 -nm gold particles, diluted 1 : 20 in TBST with 2% HSA and, for A_1R experiments, with 2 mg/mL polyethylene glycol to suppress the formation of gold particle aggregates.

The ultrathin sections were processed both with single-labelled and double-labelled procedures. In double-labelling experiments (Ottersen *et al*., 1992), sections were treated with the antibody against $P2Y_1$ (dilution as above) in the first step (followed by 10-nm gold-labelled secondary antibody) and then with the A_1R antibody (dilution as above) in the next step (revealed by 15-nm gold-labelled secondary antibody). Exposure to formaldehyde vapours (80 °C, 1 h) was used between the two immunolabelling steps (Wang & Larsson, 1985) to destroy the remaining free anti-IgG binding sites on the first primary and secondary antibodies. Potential cross-reactivity arising from the subsequent use of another secondary antibody that would be directed against the same species is prevented in this manner, allowing the simultaneous detection of two different antigens when using two primary antibodies from the same species, distinguishing the two by means of different gold particle sizes (10 nm for $P2Y_1R$, 15 nm for A_1R). The double-labelling approaches gave similar patterns as the single-labelling protocol.

Negative control experiments also were performed, replacing the incubation with the primary antibodies with 2% HSA in TBST; staining was absent on sections that had been incubated in such a solution. Ultrathin sections were contrasted in uranyl acetate and lead citrate and observed in a Philips CM100 electron microscope.

Quantitative analysis

Electron micrographs were randomly taken in the hippocampus (magnification 34 000×). Gold particles signalling both receptors ($P2Y_1R$ or A_1R) were quantified as number of gold particles/μm^2 at glutamatergic synapses (i.e. asymmetric synapses on dendritic spines) in the stratum radiatum of area CA1 and CA3, as well as in the juxtagranular part of the dentate molecular layer. The former are formed by terminals of ipsilateral (Schaffer collaterals) and commissural axon collaterals from CA3 pyramids), the latter by terminals of mossy cells in the dentate hilus. Only synapses with clearly visible postsynaptic membrane and postsynaptic density were selected for analysis; essentially all synapses with this morphology are glutamatergic in these areas (for identification criteria, see Gylterud Owe *et al*., 2005). Quantitave analyses were carried out on sections single labelled for either $P2Y_1R$ or A_1R. Specific membrane compartments were

defined and used for quantifications; they correspond to the presynaptic vesicles membranes, the membrane overlying the postsynaptic density (PSD), presynaptic membrane (opposite to the PSD), pre- and post-perisynaptic membranes (corresponding to membrane lateral to the presynaptic active zone and the PSD, extending laterally by half the length of the PSD), extrasynaptic membranes (belonging to either presynaptic terminals or postsynaptic spines/dendrites but excluding the synaptic and perisynaptic membranes), postsynaptic intracellular membranes, astroglia membranes and mitochondrial outer membranes (Fig. 1; cf. Bergersen *et al.*, 2005). In addition, gross distribution of gold particles was recorded over the following location categories; presynaptic terminal, postsynaptic spine, synaptic cleft, astrocytes, mitochondria, extracellular and undefined.

Particles located within 40 nm (perpendicular distance between the centre of gold particle and the membrane) from different membranes were recorded. This distance was chosen because 40 nm is approximately equal to the lateral resolution of the immunogold method, i.e. the maximum distance from the centre of the gold particle and the epitope, determined experimentally (Chaudhry *et al.*, 1995; Nagelhus *et al.*, 1998). The areas sampled were determined by grid point analysis (Gundersen *et al.*, 1988; Gundersen *et al.*, 1998), and the densities expressed as gold particles/μm^2. The distance between the centres of gold particles, representing receptors, and the external face of the postsynaptic density was determined along a perpendicular axis. All gold particles located within the postsynaptic spine and the presynaptic terminal were recorded; the width of the synaptic cleft was also measured. The distribution of gold particles was compared with that of grid points placed randomly over the sampled area (Gundersen, V *et al.*, 1998; Bergersen *et al.*, 2003) in order to relate the distributions of A_1R and $P2Y_1R$ to a random distribution.

Rat brain membrane lysates and Western blotting

Western blot analysis on rat hippocampus and full-brain membranes has been used to confirm the specificity of the antibodies and the presence of the receptors, as a further control.

The whole brain or the hippocampus were removed from Wistar rats (200–300 g; $n = 3$) and immediately processed, keeping on ice. The tissues were suspended in 20 volumes of ice-cold 50 mM Tris HCl, 2 mM $MgCl_2$ buffer, pH 7.4, containing EDTA 1 mM and protease inhibitors (benzamidine 0.16 mg/mL, trypsin inhibitor 0.03 mg/mL and bacitracin 0.2 mg/mL) (buffer A). The tissues were then homogenized with a Polytron homogenizer and after centrifugation (48 000 × *g* for 10 min at 4 °C), the membrane pellets were resuspended and re-homogenized in buffer A containing ADA 2 U/mL to obtain a concentration of 50 mg/mL (from original tissue weight). After incubation for 30 min at 37 °C, the samples were centrifuged at 4 °C and each pellet was resuspended to the used concentration, boiled in Laemmli solution for 5 min, centrifuged at room temperature for 5 min and the supernatant used for electrophoresis (or kept at −20 °C until use). Tissue membrane homogenates (50 µg) were then processed by immunoblot following the method

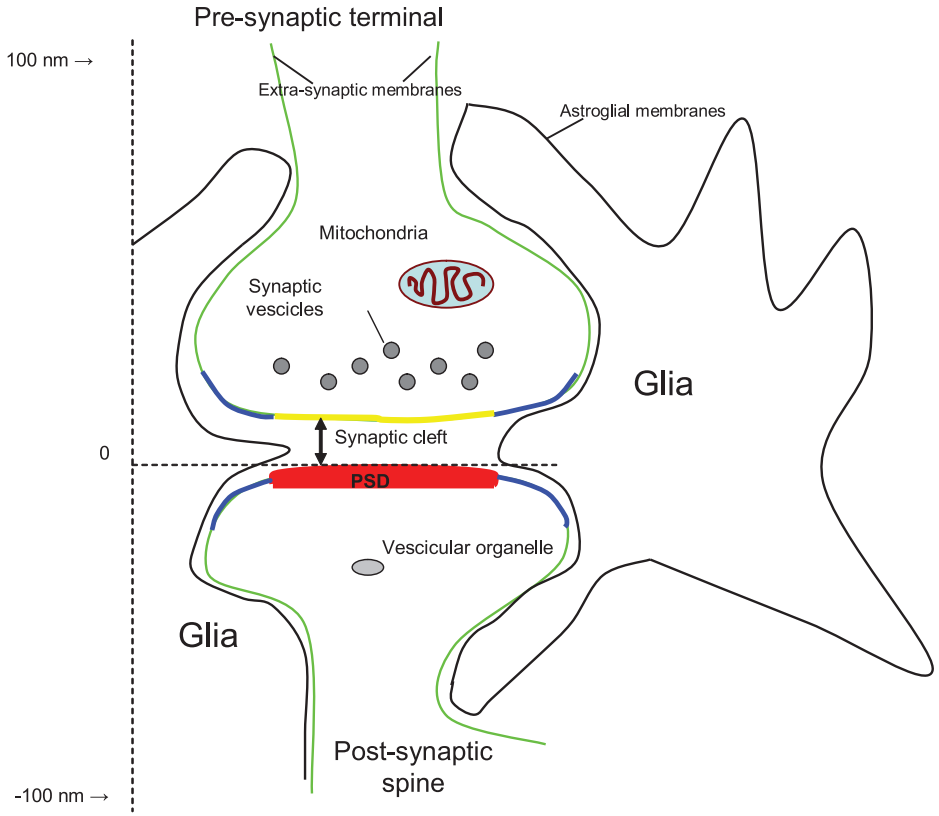

FIG. 1. Schematic illustration of a synapse between a presynaptic terminal and a dendritic spine. Analysis of gold particle density (number of gold particles/μm^2) was performed in specific membrane regions that were defined as presynaptic vesicles membranes, the postsynaptic membrane overlying the postsynaptic density (PSD; red), presynaptic membrane 'active zone' (i.e. opposite to the PSD; yellow), pre- and post-perisynaptic membranes on each side of the active zone (blue), extrasynaptic membranes (belonging to either presynaptic terminals or postsynaptic spines/dendrites but excluding the synaptic and perisynaptic membranes; green), postsynaptic intracellular membranes, astroglial plasma membranes (black) and mitochondrial outer membranes (brown). Note that the length of perisynaptic membrane considered corresponds to half the total length of the PSD, on each side (the same is valid for the presynaptic perisynaptic membrane). Figure modified from Bergersen *et al.* (2005).

previously described (Trincavelli *et al*., 2004) with minor modifications. Briefly, samples were resolved by SDS-PAGE (10%), transferred to nitrocellulose membranes and incubated with primary antibodies against A_1R (2 μg/mL) (Lasley *et al*., 2000; Ponzio & Hatton, 2005) or $P2Y_1R$ (4 μg/mL) (Wang *et al*., 2002; Franke *et al*., 2004; Franke *et al*., 2006a) overnight at 4 °C. Blots were developed using the Millipore Immobilon TM Western Chemiluminescent HRP Substrate Reagents (Millipore, MA, USA).

[^{35}S]GTPγS binding assay

For the preparation of rat HC, hippocampus from Wistar rats (200–300 g; $n = 3$) were processed essentially as described by Giuntini *et al*. (2004) and the protein concentration of the samples was determined.

A_1R coupling to G proteins was evaluated assessing the ability of the selective A_1R-agonist CHA to stimulate [^{35}S]GTPγS binding in membranes pre-treated for 10 min with buffer alone (control HC) or 100 nM MeSADP (MeSADP-treated HC). In parallel, aliquots of control membranes were pre-incubated with the A_1R selective antagonist DPCPX (50 nM) for 10 min before the CHA-stimulation.

In the same way, $P2Y_1R$/G protein coupling was evaluated assessing the ability of the agonist MeSADP to stimulate [^{35}S]GTPγS binding in membranes pre-treated for 10 min with buffer alone (control HC) or 100 nM CHA (CHA-treated HC). In parallel, control membranes were also treated with the $P2Y_1R$ selective antagonist MRS2179 (10 μM), for 10 min before MeSADP-stimulation (MRS2179-treated HC).

Aliquots of membrane homogenate (10 μg) were incubated in 0.1 mL of 25 mM Hepes NaOH, pH 7.4, 5 mM $MgCl_2$, 1 mM EDTA, 100 mM NaCl (buffer A) containing ADA (0.2 U/mL), 10 μM GDP and 0.3 nM [^{35}S]GTPγS in the presence (stimulated) and absence (basal) of a range of concentrations of CHA or MeSADP (0.1 nM–10 μM). ADA was added to the assay to eliminate the interference of endogenous adenosine in the basal [^{35}S]GTPγS binding. Incubation was carried out at 25 °C for 2 h. Unspecific binding was defined in the presence of 100 μM GTPγS; resulted in less than 10% of total binding. Binding reactions were terminated by rapid filtration under vacuum through Whatman GF/C glass fibre filters (Millipore Corporation). The filters were washed three times with 3 mL of 50 mM Tris HCl, 5 mM $MgCl_2$, pH 7.4 and then counted in a scintillation cocktail. The concentration-dependent increase in specific [^{35}S]GTPγS bindings by agonists was expressed as the per cent increase above the basal unstimulated binding (fixed as 100%). All experiments were performed in duplicate.

Data analysis

Data from immunogold cytochemistry localization were statistically analysed with one-way ANOVA and/or with Student's *t*-test (two tails, unpaired) by the computer program package GraphPad PRISM Version 4.00 (GraphPad Software, San Diego, CA, USA) and reported as mean ± SEM; statistical significance refers to results where $P < 0.05$ was obtained.

Agonist dose–response curves were analysed by the non-linear regression curve-fitting computer program GraphPad PRISM Version 4.00 and the EC_{50} values were derived. Data are reported as mean ± SEM of four different experiments (performed in duplicate). Statistical analysis (Student's *t*-test, two tails, unpaired) was performed using GraphPad PRISM; significance refers to $P < 0.05$.

Results

Immunolocalization

Postembedding immunogold electron microscopy was used to study A_1R and $P2Y_1R$ (Fig. 2A and B) in rat hippocampus, focusing on glutamatergic synapses (i.e. small terminals with asymmetric synapses on dendritic spines) and surroundings glia. For quantitative analysis single-labelled sections, were randomly selected from CA1 and CA3 stratum radiatum, and juxtagranular part of the dentate molecular layer, regions that are particularly high in nerve terminal glutamate and glutamatergic markers (e.g. Cotman *et al*., 1987). As no overt differences were noticed between the areas, they were analysed together. Both A_1R and $P2Y_1R$ were detected on synaptic and glial membranes (Fig. 2A and B). Omitting the primary antibodies abolished labelling (Fig. 2C), indicating a low unspecific signal due to the detection system.

A_1R and $P2Y_1R$ antibody specificity was addressed further by Western blot analysis, using rat whole brain and hippocampus membrane fractions (Fig. 2D and E). Results confirmed the presence of the two receptors and their antibody specificity. The A_1R immunoreactive band corresponds to the dimer form of A_1Rs (79 kDa; Fig. 2D) (Ciruela *et al*., 1995; Blum *et al*., 2002), while the $P2Y_1R$ multiline pattern shows immunoreactive bands at 76, 40 and 35 kDa, corresponding to dimeric and monomeric variants (Fig. 2E), in agreement with the literature data (Hoffmann *et al*., 1999; Waldo & Harden, 2004).

The receptor distribution and localization was quantified in different subcellular structures (Fig. 3A and B). The localization of both receptors was expressed as the area density, the number of gold particles/μm^2, in different structures in the vicinity of hippocampal glutamatergic synapses, determining the area by point analysis (Gundersen *et al*., 1988). Assuming the mitochondria do not contain the receptors, the density of gold particles over mitochondria may be taken to represent unspecific background binding of antibodies. (This may be an overestimate of background labelling, as the protein concentration in mitochondria is exceptionally high.) Both A_1R and $P2Y_1R$ were highly concentrated in the synaptic cleft area and in adjacent astrocytes, which were the only compartments significantly higher than mitochondria (Fig. 3A and B). Because the spatial resolution of our immunolabelling method is of the same order of magnitude as the distance between different compartments/membranes in the tissue, an individual gold-particle cannot be directly ascribed to any single structure. Therefore, the association of gold particles with membranes was analysed in several different ways.

First, we investigated the distribution of gold particles associated with each kind of cellular membrane, in the vicinity of hippocampal synapses, recording only particles within a distance equal to 10 nm from each kind of membrane to minimize 'cross firing' effects from immunoreactivity in nearby structures. Immunogold single-labelling of hippocampal sections showed that A_1R (Fig. 4A) as well as $P2Y_1R$ (Fig. 4B) are mainly associated with presynaptic membranes, postsynaptic membranes overlying the PSDs, and astroglial membranes. The high A_1R presence on presynaptic-perisynaptic membranes ($P < 0.05$, one-way ANOVA, value vs. mitochondria) could be influenced from receptors that are located in the active zone or as 'reserve' (Rebola *et al*., 2003); anyway the values on perisynaptic and extrasynaptic membranes, both pre- and post-, can be influenced from receptors that are instead on astroglia membranes, for the tight contact between these and neurons. No other columns differed from the background level, as indicated by the density of gold particles over mitochondrial outer membranes ($P > 0.05$, one-way ANOVA). Further,

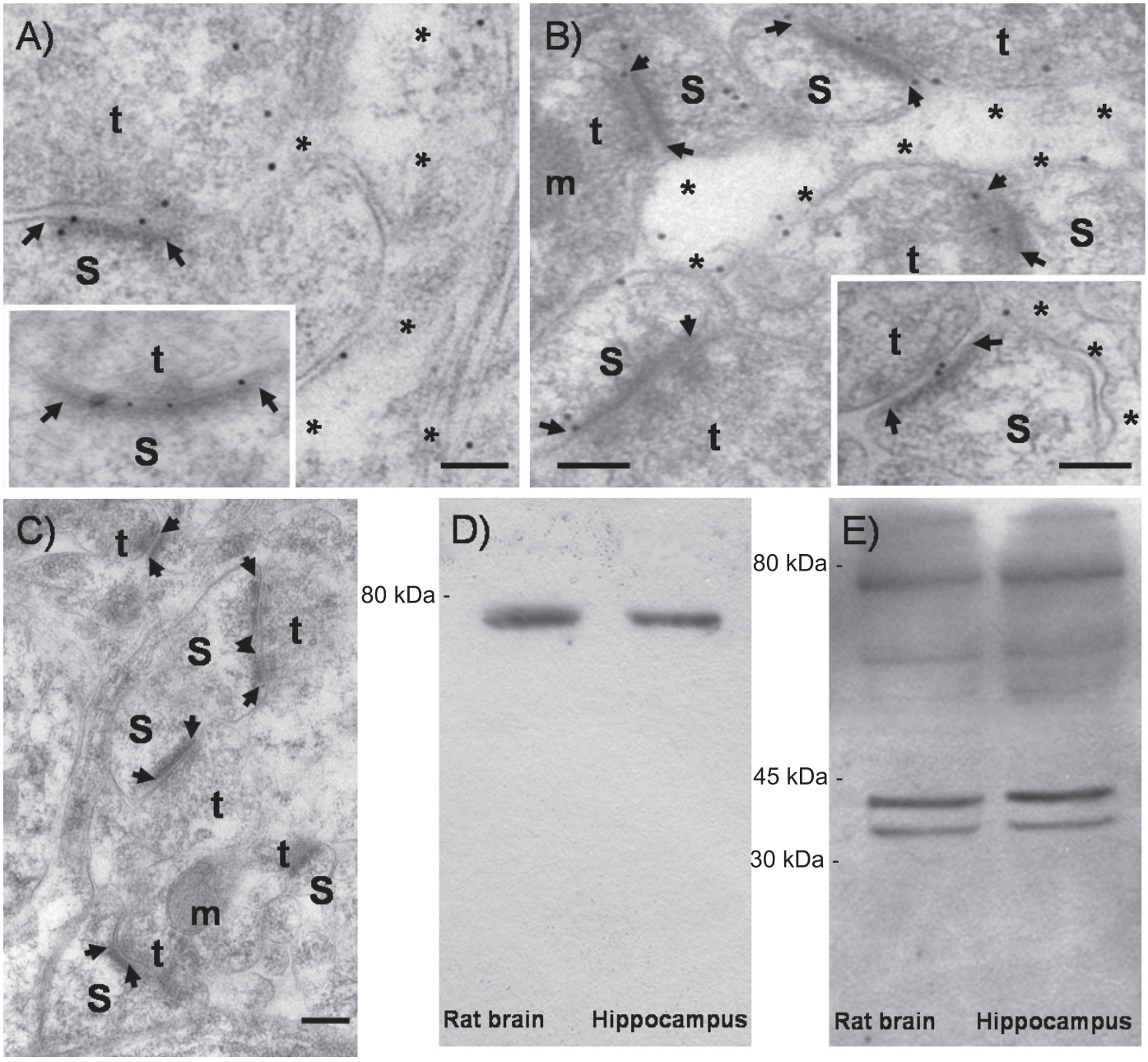

FIG. 2. Localization of purinergic receptors in glutamatergic synapses in rat hippocampus by immunogold labelling. Electron micrographs of sections single labelled for A_1R (A) and for $P2Y_1R$ (B) are illustrated by examples from CA1 stratum radiatum (A main picture, B inset), CA3 stratum radiatum (A inset) and area dentata (B main picture). Note that both A_1R and $P2Y_1R$ were detected on synaptic and glial membranes; both over the postsynaptic density (black arrows) and over the presynaptic (active zone) membranes at glutamatergic synapses and in glia (*). (C) Omission of primary antibody prevented all gold labelling (picture from CA3 stratum radiatum). Scale bar, 100 nm. m, mitochondria; S, postsynaptic dendritic spine; t, presynaptic axon terminal; *, astroglia. (D and E) Western blot analysis of A_1R (D) and $P2Y_1R$ (E), in rat whole brain and hippocampus membrane homogenates. Rat tissue membranes were lysed, proteins were separated by 10% polyacrylamide SDS-PAGE and probed with the anti-A_1R and anti-$P2Y_1R$ antibodies used for immunocytochemistry.

values at the presynaptic membrane and at the membrane covering the PSD were significantly different compared to all other locations, confirming that A_1Rs are associated with these membranes.

We then compared the distribution of gold particles representing A_1R and $P2Y_1R$ with the distribution of points spread randomly over the pictures (Fig. 5). The gold particles/random points ratio was determined at different distances, from different membrane domains, sorted into bins (10-20-30-40 nm). For the shortest distance (10 nm) bins, the highest ratio values (approximately 2) were obtained, for both A_1R and $P2Y_1R$, at presynaptic active zone membranes, postsynaptic membranes overlying the PSD and astroglial membranes (Fig. 5A and B), i.e. the same membrane domains that show the highest labelling according to the analysis of Fig. 4. Also several other neuronal membranes, but not mitochondrial outer membranes, had ratios higher than one, consistent with a moderate enrichment of receptors in them. As previously noted, the densities in perisynaptic and extrasynaptic membranes could be influenced from gold particles in active zone or in astroglial membranes.

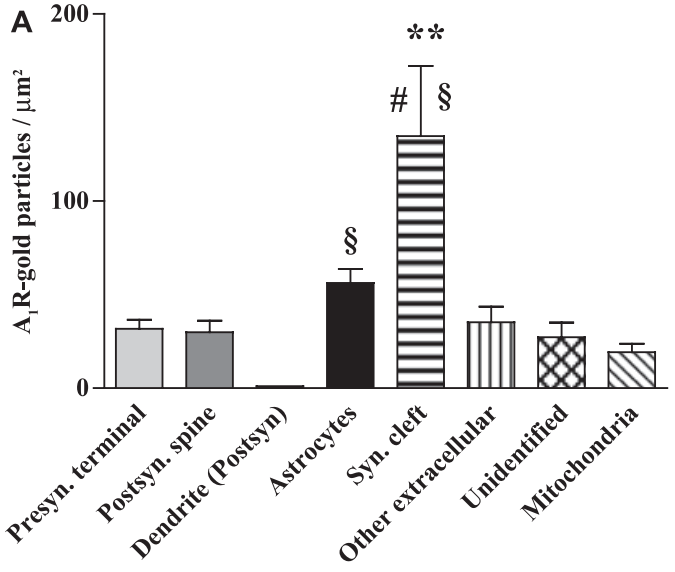

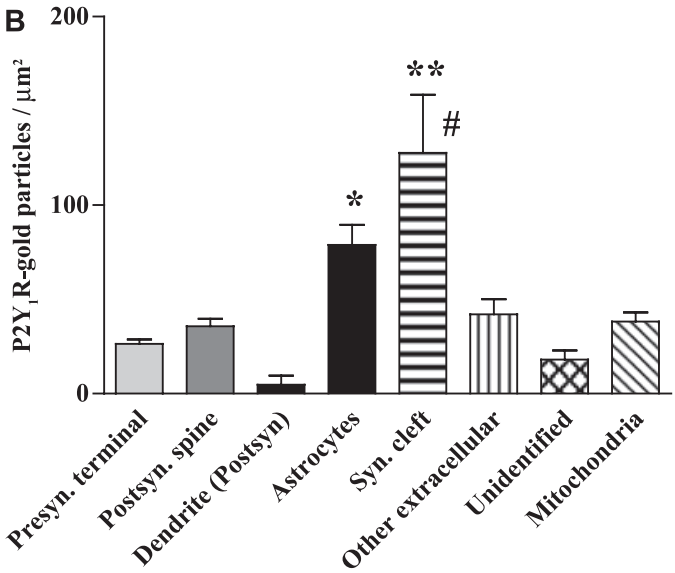

FIG. 3. Distribution of immunogold particles indicating A_1R (A) or $P2Y_1R$ (B) in different intra- and extracellular compartments. Note that both receptors are enriched at synapses and astroglia, compared to all other compartments. Data, from single labelling experiments, report the localization of receptors as the density (gold particles/μm^2; mean ± SEM) in the different compartments in the vicinity of hippocampal glutamatergic synapses (i.e. asymmetric synapses on spines, see Materials and methods; randomly selected, from $n = 3$ animals; five grids analysed for A_1R and six grids for $P2Y_1R$); the areas of the compartments were measured by point analysis (see Materials and methods). The numbers of gold particles on each structure are, in order 323, 230, 1, 52, 24, 31, 15 for A_1R; 330, 311, 5, 112, 35, 31, 32 for $P2Y_1R$. Areas analysed for each compartment are, in order 10.8, 7.7, 0.1, 1.1, 0.2, 0.6, 1.3, 1.0 μm^2 for A_1R, 12.1, 8.8, 0.2, 2.1, 0.2, 0.9, 1.7, 0.8 μm^2 for $P2Y_1R$. (A) A_1R. $^{**}P < 0.01$, one-way ANOVA, all compartments compared to mitochondria (Dunnett's multiple comparison test). Synaptic cleft is significantly different compared to all other domains ($^{\#}P < 0.01$, one-way ANOVA, Tukey's multiple comparison test). Astrocytes and synaptic cleft columns showed higher receptor density ($^{\S}P < 0.05$, Student's *t*-test, two-tails, unpaired) compared to mitochondria. (B) $P2Y_1R$; $^{*}P < 0.05$, $^{**}P < 0.01$ all domains compared to mitochondria, one-way ANOVA (Dunnett's multiple comparison test). Synaptic cleft is significantly different compared to all other domains ($^{\#}P < 0.001$ vs. all except astrocytes, $P < 0.01$ vs. astrocytes, One-way ANOVA, Tukey's multiple comparison test).

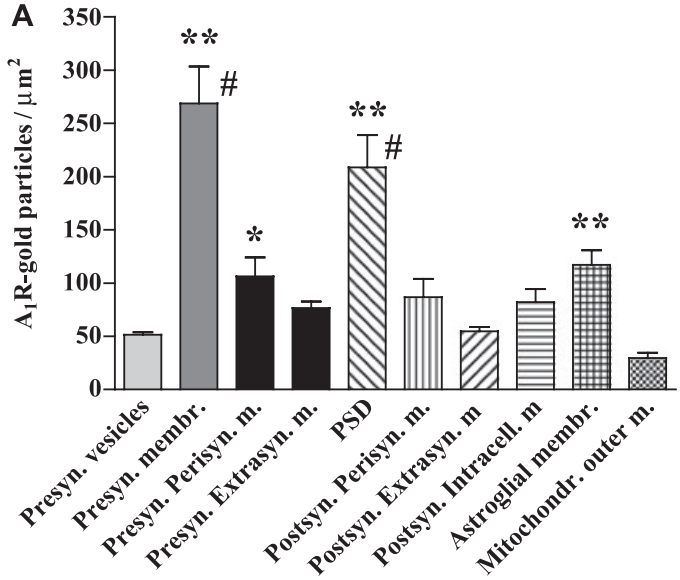

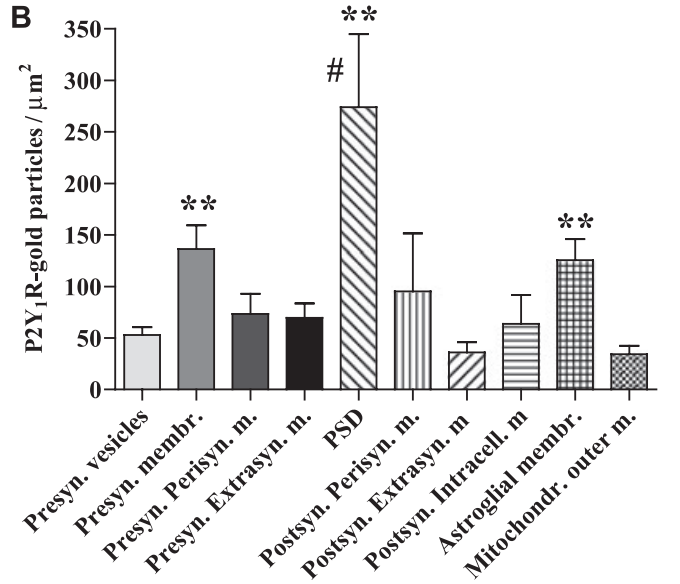

FIG. 4. Distribution of immunogold particles indicating A_1R (A) or $P2Y_1R$ (B) over different categories of cellular membranes in the vicinity of hippocampal synapses. Both receptor types are enriched over presynaptic as well as postsynaptic membranes and over astroglial membranes. Only particles located within a distance equal to 10 nm from each kind of membrane were recorded, to minimize 'cross firing' effects from immunoreactivity in nearby structures. The data are presented in the same way, and are from the environments of the same synapses, as are the data in Fig. 3. The sizes of the areas sampled for gold particles (± 10 nm on each side of the membrane) were determined by point analysis. Areas analysed for each category are, in order 3.8, 0.5, 0.3, 1.4, 0.7, 0.3, 1.1, 0.3, 0.6, 0.6 μm^2 for A_1R; 5.1, 0.8, 0.3, 1.6, 0.8, 0.4, 2.0, 0.6, 1.2, 0.7 μm^2 for $P2Y_1R$. The numbers of gold particles within 10 nm from each membrane column are, in order 196, 126, 22, 98, 141, 19, 54, 32, 57, 12 for A_1R.; 260, 81, 15, 101, 124, 26, 74, 36, 116, 27 for $P2Y_1R$. The density of gold particles over the outer membrane of mitochondria gives an estimate of the background level. (A) $^{*}P < 0.05$, $^{**}P < 0.01$, all columns compared to mitochondria background level, one-way ANOVA (Dunnett's multiple comparison test). Presynaptic membrane and PSD are significantly different compared to all other membrane categories ($^{\#}P < 0.01$, one-way ANOVA, Tukey's multiple comparison test). (B) $^{**}P < 0.01$, all columns compared to mitochondria background level, one-way ANOVA (Dunnett's multiple comparison test). PSD is significantly different compared to all other columns except for presynaptic membranes and astroglial membranes ($^{\#}P < 0.01$, one-way ANOVA, Tukey's multiple comparison test).

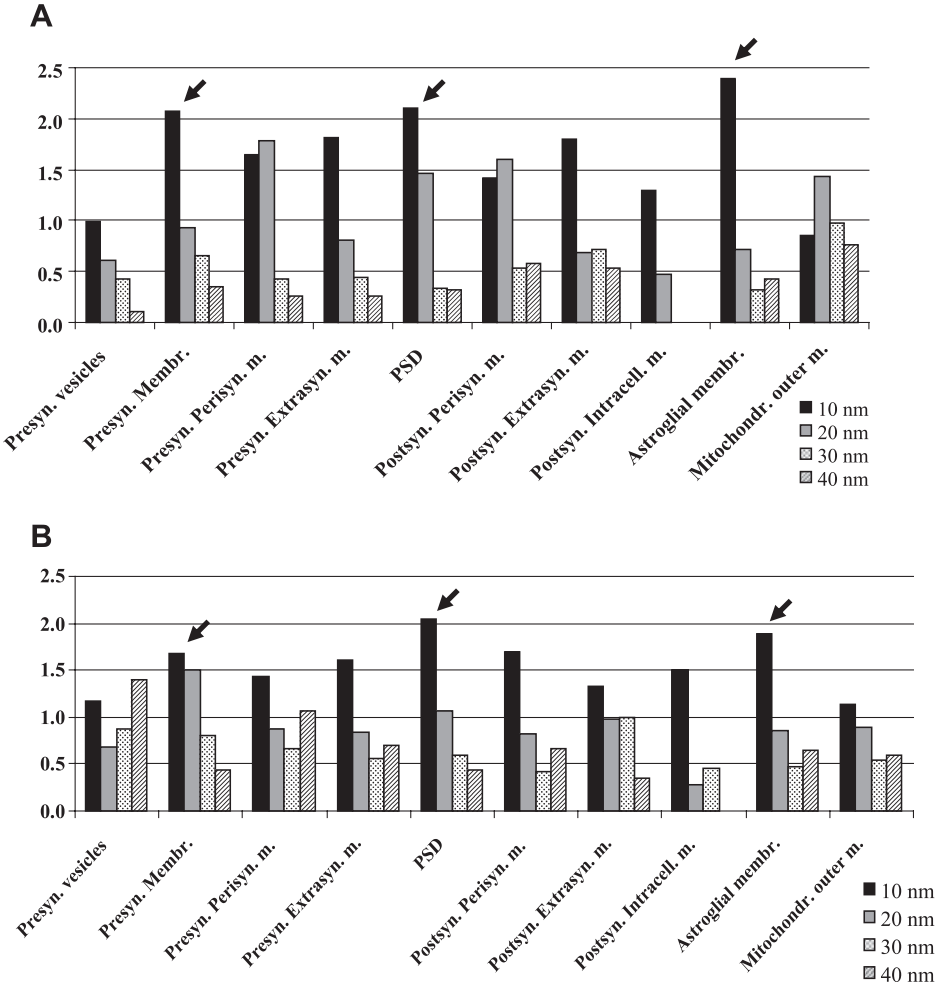

FIG. 5. Histogram of gold particles/random points ratio; gold particles were grouped in bins depending the distance (10, 20, 30, 40 nm) from each kind of membrane, at hippocampal glutamatergic synapses and surrounding glia. The percentage of the total number of gold particles that occurred in each bin was divided by the percentage of the total random points (within 40-nm distance) that occurred in the same bin; the ratio gives the distribution of receptors relative to a random distribution. A ratio > 1 for the shorter distance bins (10 nm and 20 nm), indicates a close association with the membrane observed. Note the higher ratios (arrows) for short distances at presynaptic active zone membranes, postsynaptic membranes overlying the PSD and astroglial membranes, for both A_1R (A) and $P2Y_1R$ (B).

The average distance of immunogold particles from membranes was then measured and compared with a random distribution (Fig. 6). Note that for both A_1R (Fig. 6A) and $P2Y_1R$ (Fig. 6B) the mean distance of gold particles is shorter than that of random points in all membranes, except in mitochondrial outer membranes (which represent an estimate of background labelling).

To dissect further the synaptic localization of A_1R and $P2Y_1R$, all the hippocampal glutamatergic synapses previously analysed were processed to record the percentage distribution of both receptors as a function of the perpendicular distance from the postsynaptic membrane overlying the PSD (Fig. 7). The percentage distribution of A_1Rs in the synaptic area (Fig. 7A, left) showed that A_1R are located over both the PSD and the presynaptic membrane, although the density is highest over the latter. The influence of the extracellular location of the epitope recognized by the A_1R antibody may have contributed to the high level of gold particles located in the synaptic cleft. A_1R-gold particles situated over the synaptic cleft were preferentially associated with the presynaptic membrane (Fig. 7A, right), indicating a shared distribution of the receptor between the presynaptic and postsynaptic sides. $P2Y_1Rs$ were relatively more distributed towards the PSD membrane (Fig. 7B, left), compared to A_1Rs, and gold particles in the cleft showed less enrichment on the presynaptic side (Fig. 7B, right). These results are consistent with a high degree of co-localization of the two types of receptor, but with relatively less of $P2Y_1R$ than of A_1R on the presynaptic side.

In conclusion, A_1R and $P2Y_1R$ are co-localized in synaptic and astroglial membranes in glutamatergic synapses and surrounding glial membranes in the hippocampus. The quantitative analyses of single-labelling data were confirmed by the qualitative analysis of double-labelling experiments (Fig. 8). The double-labelling approach gave similar patterns as the single labelling protocol; the receptors were detected together in the same structures and both were associated with synaptic and astroglial membranes (Fig. 8).

Functional assays

The effect of $P2Y_1R$ activation on A_1R/G protein coupling was measured in HC by evaluating the ability of the A_1R agonist CHA to stimulate G protein activation following 100 nM MeSADP pre-incubation (for 10 min). In control HC, CHA stimulated G protein activation with an EC_{50} of 30.60 ± 3.99 nM (Fig. 9). To test the CHA-mediated selective A_1R activation in our model, we also stimulated

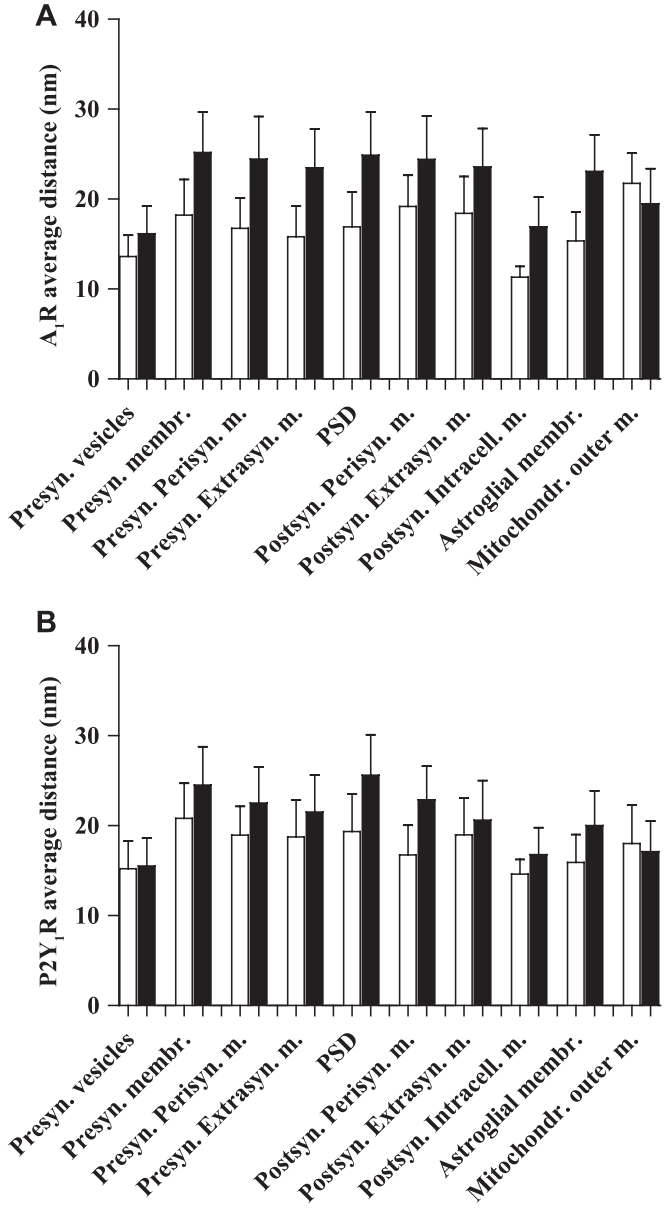

FIG. 6. Average distances of immunogold particles from membranes. The values are the mean ± SEM of the distances of gold particles (white bars) or random points (black bars) located within a distance equal to 40 nm from different membrane categories, in the vicinity of glutamatergic synapses in rat hippocampus. Note that for both A_1R (A) and $P2Y_1R$ (B) the mean distance of gold particles is shorter than that of random points in all membranes, except in mitochondria outer membranes (which represent background labelling). The total number of particles counted is for A_1R gold particles 286, 241, 34, 159, 230, 38, 101, 37, 91, 241; for $P2Y_1R$ gold particles 392, 238, 41, 183, 247, 47, 145, 44, 207, 44; for A_1 random points 457, 212, 46, 313, 218, 48, 187, 39, 149, 177; for $P2Y_1$ random points 457, 127, 47, 270, 132, 55, 269, 60, 162, 63.

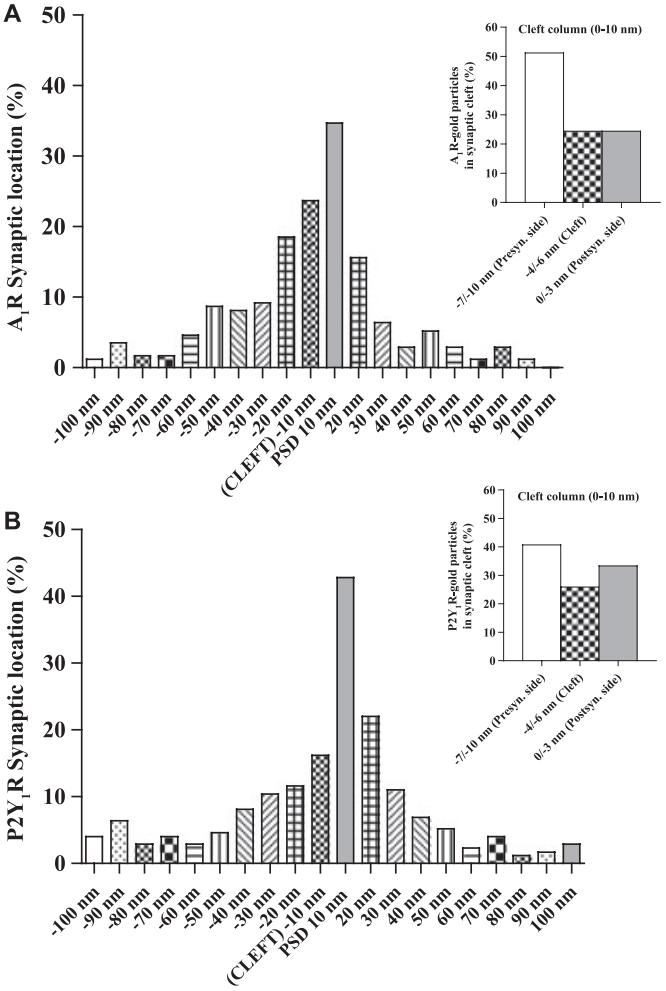

FIG. 7. Distribution of immunogold particles across the synaptic cleft. The histograms on the left show the percentage of gold particles representing A_1R (A) and $P2Y_1R$ (B) in the synaptic area, as a function of the distance up to 100 nm from the postsynaptic membrane at the PSD. The distance between the centre of gold particles and the external face of the PSD was determined along a perpendicular axis (cf. Fig. 1). Positive columns (10 to 100 nm) represent the postsynaptic spine; negative columns (−20 to −100 nm) the presynaptic terminal; the −10 nm column represents the synaptic cleft (i.e. position 0 to −10 nm). The actual width of the synaptic cleft was 11.5 ± 0.4 nm (average ± SEM, $n = 79$). Numbers of gold particles considered in the analysis are $n = 266$ for A_1R; $n = 296$ for $P2Y_1R$. All synapses previously analysed have been processed in this analysis. Note that the highest particle counts for A_1R as well as $P2Y_1R$ were in the PSD bin. The histograms on the right show the distribution of immunogold particles within the synaptic cleft. The percentage of the total number of gold particles located in the synaptic cleft ($n = 41$ for A_1R; $n = 28$ for $P2Y_1R$), in function of the distance from the outer face of the PSD; presynaptic side, position between 0 and −3 nm; postsynaptic side, between −6 and −10 nm; middle of cleft, between −3 and −6 nm. The distributions within the synaptic cleft indicate that both A_1R (A) and $P2Y_1R$ (B) are located presynaptically as well as postsynaptically.

HC in the presence of the selective A_1R antagonist DPCPX (50 nM; pre-incubated for 10 min). DPCPX prevented CHA-mediated G protein coupling in HC (Fig. 9), showing that the G protein activation is selectively driven by A_1R. The CHA-mediated effect was abolished in the presence of the selective A_1R antagonist DPCPX (50 nM), confirming A_1R specific activation.

Membrane pre-incubation with 100 nM MeSADP induced a right-shift of the CHA dose/response curve (EC_{50} = 106.26 ± 16.39 nM), suggesting a significant impairment in A_1R-G protein coupling when $P2Y_1$ receptor is activated (*t*-test, two-tails, unpaired $P = 0.004$ for EC_{50} of MeSADP-treated HC vs. control HC; Fig. 9).

On the other hand, the A_1R activation effect on $P2Y_1R$/G protein coupling was measured by evaluating the ability of the $P2Y_1R$ agonist MeSADP to stimulate G protein activation in the absence or the presence of 100 nM CHA (pre-incubated for 10 min). In control HC,

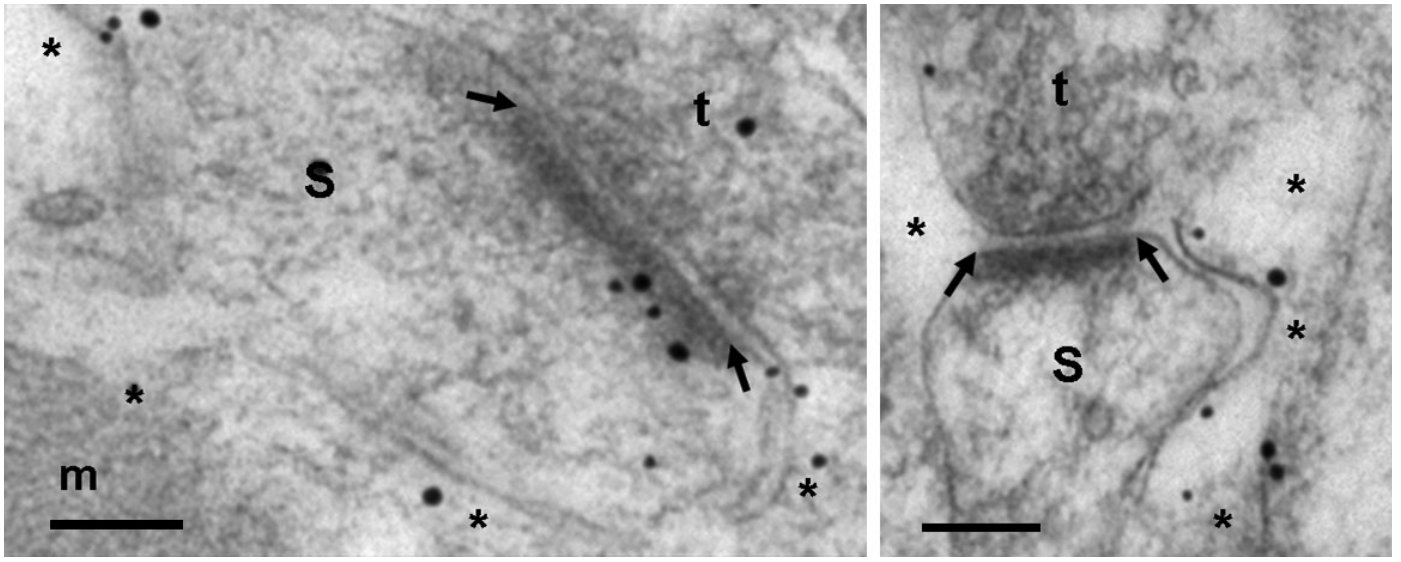

FIG. 8. Qualitative co-localization of $P2Y_1R$ and A_1R in glutamatergic synapses (randomly selected) and surrounding glia, in rat hippocampus CA3 stratum radiatum. Electron micrograph of a section double labelled for A_1R (large gold particles, 15 nm) and $P2Y_1R$ (small gold particles, 10 nm). The double-labelling approach gave similar patterns as the single-labelling protocol. Note that the receptors were detected together in the same structures. A_1R and $P2Y_1R$ appeared co-localized (qualitative data) on the PSD (black arrows) and on astroglia (*). Scale bar, 100 nm. M, mitochondria; S, postsynaptic spine; t, presynaptic terminal; *, astroglia.

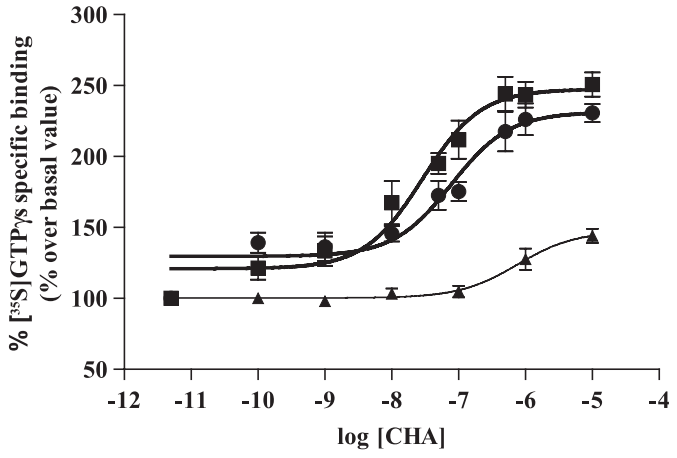

FIG. 9. Effect of $P2Y_1R$ activation on A_1R agonist-mediated G protein coupling. Dose–response curves of CHA-stimulated [^{35}S]GTPγS binding were obtained incubating control HC (■) and MeSADP-treated (100 nM) HC (●) with different agonist concentration (0.1 nM−10 μM). Data are expressed as percentage of [^{35}S]GTPγS specific binding over basal value, set to 100%, and are reported as mean ± SEM ($n = 4$), all performed in duplicate. Student's *t*-test, two-tails, unpaired: $P = 0.004$ for EC_{50} of Control HC vs. MeSADP-treated HC. Aliquots of HC were also pre-exposed to the selective A_1R antagonist DPCPX (50 nM; ▲) and then stimulated by CHA (0.1 nM−10 μM).

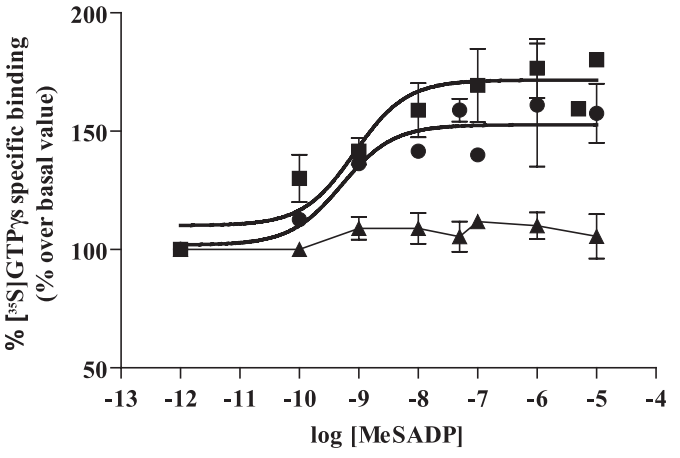

FIG. 10. Effect of A_1R activation on $P2Y_1R$ agonist-mediated G protein coupling. Dose–response curves of MeSADP-stimulated [^{35}S]GTPγS binding were obtained incubating control HC (■) and CHA-treated (100 nM) HC (●) with different agonist concentration (0.1 nM−10 μM). Data are expressed as percentage of [^{35}S]GTPγS specific binding over basal value set to 100% and are reported as mean ± SEM ($n = 4$), all performed in duplicate. Student's *t*-test, two-tails, unpaired: $P = 0.03$ for EC_{50} of control HC vs. CHA-treated HC. Aliquots of HC were also pre-exposed to the selective $P2Y_1R$ antagonist MRS2179 (10 μM; MRS2179-treated HC; ▲) and then stimulated by MeSADP (0.1 nM−10 μM). Data are expressed as percentage of [^{35}S]GTPγS specific binding over basal value set to 100% and are reported as mean ± SEM ($n = 4$), all performed in duplicate.

MeSADP stimulated [^{35}S]GTPγS binding with an EC_{50} of 0.851 ± 0.147 nM (Fig. 10).

To test the selectivity of MeSADP for $P2Y_1$ receptor subtype in our model, we also stimulated HC in the presence of the selective $P2Y_1R$ antagonist 10 μM MRS2179 (pre-incubated for 10 min). MRS2179 blocked MeSADP-mediated G protein coupling in HC (Fig. 10), showing this G protein activation is selectively driven by $P2Y_1R$, and other P2Y receptors sensitive to MeSADP ($P2Y_{12-13}$) have no significant signal component in rat hippocampus. Membrane CHA pre-incubation induced a significant increase in MeSADP potency to activate $P2Y_1R$-G protein coupling, with an EC_{50} of 0.393 ± 0.058 nM (*t*-test; two-tails, unpaired $P = 0.03$ vs. control HC), without significantly affecting the G protein coupling efficacy level of the agonist dose/response curve (Fig. 10).

Cell treatment with MeSADP or CHA induced an increase in the basal [^{35}S]GTPγS binding value, thus suggesting the agonists affect the G protein activation state. Values are reported as fmol/mg of proteins; control HC = 183.96 ± 30.2; MeSADP HC = 298.65 ± 30.18; CHA

HC = 317.93 ± 8.42 (*t*-test, two-tails, unpaired, $P = 0.047$ for Me-SADP-treated HC vs. control HC; $P = 0.017$ for CHA-treated HC vs. control HC).

Discussion

Localization and co-localization

This is the first study on A_1R and $P2Y_1R$ localization and co-localization in hippocampus by postembedding immunogold electron microscopy analysis. This high resolution technique is able to show the precise subcellular localization of receptors in different subcellular compartments and cell populations (e.g. Bergersen *et al*., 2003). The purinergic receptors proved to be mainly associated with membrane domains. Single-labelling immunolocalization data showed a significant enrichment of both A_1R and $P2Y_1R$ mainly in postsynaptic membranes at the PSD, in presynaptic active zones, and in astroglial membranes at glutamatergic synapses and surrounding glia in the rat hippocampus. The same conclusion was arrived at by analysing the data in different ways, in order to partly overcome the limits posed by 'cross firing' effects antigen located in closely spaced neighbouring membranes. Because of these, the exact labelling densities of the individual membranes cannot be determined. While the three membrane categories mentioned contain higher levels of both of the purinergic receptors studied, low or moderate labelling may exist in other membrane categories. The data suggest that there may be relatively higher densities of A_1R than of $P2Y_1R$ at the presynaptic compared to the postsynaptic membrane. Part of this observed difference might be attributable to the fact that the antibodies were to extracellular and intracellular epitopes, respectively, although the inner and outer surfaces of the plasma membrane are only 4–5 nm apart, i.e. an order of magnitude less than the lateral resolution of the immunogold method. However, the main conclusion is that the two receptor types are similarly distributed, compatible with a high degree of co-localization. This was born out by double-labelling experiments that showed A_1R and $P2Y_1R$ to be closely spaced along synaptic and glial membranes.

In parallel, the specificities of A_1R and $P2Y_1R$ antibodies used in immunohistochemistry, were assessed by immunoblotting assay using rat whole brain and hippocampus membrane fractions. The obtained results were according to literature data (Hoffmann *et al*., 1999; Blum *et al*., 2002; Moore *et al*., 2002; Waldo & Harden, 2004) and confirmed that antibodies selectively recognized A_1 and $P2Y_1$ receptors in hippocampal membranes.

Our high resolution data serve to extend and reconcile previous reports obtained with lower resolution methods. Thus A_1R immunoreactivity has been reported in hippocampus both at presynaptic and postsynaptic terminals but not at glial cells (Ochiishi *et al*., 1999); an immunohistochemical study in the rat hippocampus has concluded that A_1Rs were mostly located in axons rather than in nerve terminals (Swanson *et al*., 1995), whereas work on synaptosomal fractions (Rebola *et al*., 2003) has suggested that A_1Rs are enriched in nerve terminals and are mainly located in synapses, both in the presynaptic active zone and in the PSD membranes. $P2Y_1R$ immunoreactivity has been found in astroglia and in different kinds of neurons in hippocampus (Moran-Jimenez & Matute, 2000), especially in ischemic sensitive areas while at the same time another study reported a striking neuronal localization for $P2Y_1R$ (human brain, Moore *et al*., 2000). $P2Y_1Rs$ have been reported to be present and active on astrocytes all around the brain (Franke *et al*., 2001; Volonte *et al*., 2006). A high degree of co-localization of A_1R and $P2Y_1R$ has been found in rat hippocampus by immunofluorescence experiments but without cellular and subcellular identification (Yoshioka *et al*., 2002).

We studied A_1Rs and $P2Y_1Rs$ in the hippocampal region considering the fact that the hippocampus has been identified as a major target site for numerous disease processes (Bachevalier & Meunier, 1996; Harry & Lefebvre d'Hellencourt, 2003), and considering the generally assumed involvement of purinergic receptors in pathophysiological mechanisms and in the modulation of brain damage (Fredholm, 1997; Franke *et al*., 2006b). Ischemia, to which hippocampus is particularly vulnerable, produces a marked increase in glutamate within the brain extracellular space (Benvensiste *et al*., 1984; Hagberg *et al*., 1985), thereby triggering excitotoxic injuries (Choi & Rothman, 1990). Because of the importance of glutamate in pathological conditions and because its release, in neurons and in astrocytes, is modulated both through A_1R (Rudolphi *et al*., 1992; Masino *et al*., 2002) and $P2Y_1R$ (Rodrigues *et al*., 2005; Franke *et al*., 2006a; Jourdain *et al*., 2007), the present study was focused on A_1R–$P2Y_1R$ localization and co-localization within and in the vicinity of glutamatergic synapses.

Our results provide direct morphological support for the previous suggestions that both of these receptors contribute to and interact in the modulation of glutamate release (Rudolphi *et al*., 1992; Mendoza-Fernandez *et al*., 2000; Masino *et al*., 2002; Kawamura *et al*., 2004; Rodrigues *et al*., 2005).

Functional interaction

The functional interaction of A_1Rs and $P2Y_1Rs$ suggested by the morphological observations was subsequently confirmed through measurement of G protein activation initiated by the A_1R agonist, CHA, or the $P2Y_1R$ agonist, MeSADP, respectively, and modification of the response through pre-incubation with the other agonist. Because the receptors on study are coupled to different G protein subtypes (Munshi *et al*., 1991; Yoshioka & Nakata, 2004) and to different intracellular signalling pathways, the [^{35}S]GTPγS binding method was chosen to investigate the A_1R–$P2Y_1R$ interaction and their reciprocal modulation at the membrane level, allowing any change in their functioning to be determined independently of the second messenger systems activated (Lorenzen *et al*., 1996).

According to literature data (Gao *et al*., 2003; Dixon *et al*., 2004; Niebauer *et al*., 2005), the selected agonist pre-incubation times and concentrations pre-stimulating A_1R and $P2Y_1R$ (100 nM CHA and 100 nM MeSADP, respectively) allow a selective and maximal receptor activation.

The EC_{50} for CHA in stimulating A_1R-G protein coupling was around 30 nM. Although CHA has been reported to block [^{3}H]DPCPX binding at A_1R with a K_i of approximately 5 nM in rat hippocampus (Maemoto *et al*., 1997), according to our data, higher EC_{50} values for different A_1R agonists in the [^{35}S]GTPγS binding assay have been found (Lorenzen *et al*., 1996; Cordeaux *et al*., 2004). In order to obtain a selective stimulation of A_1R, without interference of other receptor subtypes, we have chosen treatment of hippocampal membranes with 100 nM agonist CHA. In fact in hippocampus, although A_1Rs are the mainly expressed adenosine receptors, the presence of low amounts of A_{2A} and A_3 receptors have been described (Duarte *et al*., 2006; Lopes *et al*., 2003). Nevertheless, these receptors have a different agonist pharmacological profile; CHA, in fact, shows a high affinity towards A_1Rs (Murphy & Snyder, 1982; Maemoto *et al*., 1997) and a low affinity towards A_{2A} ones (Cunha *et al*., 1996; Gao *et al*., 2003). Even if, in our experimental conditions, the EC_{50} for CHA in stimulating A_1R-G-protein coupling was around 30 nM, the

real binding potency of CHA to A_1R sites is around a few nanomolar units or indeed in the subnanomolar range in rat hippocampus, so the agonist at 100 nM is able to selectively saturate A_1R binding sites. This was confirmed by an antagonist dose–response curve, DPCPX was able to completely abrogate the effects mediated by CHA from 1 to 100 nM. At higher agonist concentrations the antagonistic effect of DPCPX was reduced suggesting that the agonist binds to a different receptor population, probably identifiable with A_{2A} receptor sites.

On the other hand, in our results, MeSADP showed subnanomolar potency in stimulating $P2Y_1R$. Because of the absolute potency of nucleoside tri- and diphosphates for P2Y receptors is dependent on the levels of receptor protein expression, typical EC_{50} values are not easily defined for specific agonists at particular P2Y receptor subtypes in different tissue preparations and cell lines (Volontè *et al*., 2006). In accordance with our results, low nanomolar and subnanomolar EC_{50} values have been reported for MeSADP towards human $P2Y_1R$, expressed in astrocytoma 1321 N1 cells (Palmer *et al*., 1998; Niebauer *et al*., 2005), and rat $P2Y_1R$, expressed in HEK 293 cells (Vohringer *et al*., 2000).

MeSADP is the principal agonist not only at $P2Y_1R$ but also at $P2Y_{12-13}$ receptors, that are coupled to G_I proteins and are expressed (mRNA) in the brain (Hollopeter *et al*., 2001; Zhang *et al*., 2002; Sasaki *et al*., 2003), even if not at high level in the hippocampus (Fumagalli *et al*., 2004; Amadio *et al*., 2006). To confirm that in our model the MeSADP-mediated G-protein activation was mainly driven by $P2Y_1R$, we also stimulated hippocampal membranes in the presence of the selective $P2Y_1R$ antagonist, MRS2179. MRS2179 was able to block the MeSADP-mediated response, confirming the $P2Y_1R$ involvement as no antagonistic effects have been demonstrated on $P2Y_{12-13}$ receptors at the MRS2179 concentrations used (Moro *et al*., 1998; Von Kugelgen, 2006).

The results obtained on A_1R–$P2Y_1R$ cross-talk in hippocampus showed that, stimulating one receptor, the functioning of the other was changed. In particular, $P2Y_1R$ pre-activation caused an impairment in A_1R–G protein coupling with a reduction in A_1R agonist potency; on the other hand, A_1R pre-activation induced an increase in $P2Y_1R$ functional coupling to G proteins. Our results are in agreement with the previously reported reduction in the A_1R ligand affinities in cells co-expressing both A_1R and $P2Y_1R$ (Yoshioka *et al*., 2001). Various studies have reported that ATP, massively released after brain damage, acts to modulate not only its own $P2Y_1R$ but also A_1R (Hourani *et al*., 1991; Piper & Hollingsworth, 1996; Masino *et al*., 2002; Fredholm *et al*., 2003; Yoshioka & Nakata, 2004).

The functional consequence of this A_1–$P2Y_1$ receptor cross-talk is complicated by the availability time and the balance of their endogenous ligands. Extracellular ATP, rapidly available due to direct release into the extracellular space, and adenosine, available after ATP breakdown, are tightly regulated by rapid metabolism and re-uptake (Zimmermann, 2000) and can be differently regulated in physiological or pathological conditions; in fact the ecto-nucleotidase chain has proved to be up-regulated in ischemically damaged tissues (Braun *et al*., 1998).

Data, at present, have shown the A_1R–$P2Y_1R$ interaction mechanism may be used to fine-tuning the purinergic signalling, including the inhibition of neurotransmission (Nakata *et al*., 2004). Considering the new information available and the A_1R and $P2Y_1R$ involvement in glutamatergic transmission modulation (Mendoza-Fernandez *et al*., 2000; Masino *et al*., 2002; Kawamura *et al*., 2004; Rodrigues *et al*., 2005), we can speculate that there is an A_1R–$P2Y_1R$ cross-talk in rat hippocampal glutamatergic synapses and surroundings glia, where these receptors are co-localized. This might therefore be one of the mechanisms for the adenine nucleotide-mediated inhibition of glutamatergic neurotransmitter release. Therefore, as suggested for adenosine A_1 and A_{2A} receptors in striatal (Ciruela *et al*., 2006) and hippocampal (Rebola *et al*., 2005) glutamatergic nerve terminals, a cross-talk/heteromerization of A_1R–$P2Y_1R$ could exert a fine-tuning modulation of glutamatergic neurotransmission, providing a switch mechanism by which low and high concentrations of adenosine or purines could regulate glutamate release.

Because of the high level of complexity of purinergic receptor signalling (Volontè *et al*., 2006) and the regulation of glia–neuron and glia–glia communications by extracellular purines (Franke *et al*., 2006b; Jourdain *et al*., 2007), the present work opens the way to further investigation of the A_1R–$P2Y_1R$ system interaction on astrocyte cell populations, which communicate bi-directionally with neurons (Newman, 2003; Bezzi *et al*., 2004; Jourdain *et al*., 2007) and contribute to damage or to regeneration after CNS injury (Franke *et al*., 2001; Anderson *et al*., 2003).

Acknowledgements

This work has been supported by a grant from the EU Marie Curie Fellowship Program [Marie Curie Training Site on Basic mechanisms of amino acid neurotransmission (BAMAN)], from the Italian Ministero dell'Università e della Ricerca Scientifica (MURST) (COFIN 2004 on 'Purinergic receptors and neuroprotection') and from the Research Council Norway (NFR).

Abbreviations

A_1R, adenosine receptor A_1; ADA, adenosine deaminase; CHA, N^6-cyclohexyladenosine; DPCPX, 8-cyclopentyl-1,3-dipropylxanthine; GPCR, G protein coupled receptors; GTPγS, guanosine-5′-(γ-thio)triphosphate; HSA, human serum albumin; HC, hippocampal membranes; MeSADP, 2-methylthio-adenosine 5′-diphosphate; MRS2179, 2′-deoxy-N^6-methyl adenosine 3′,5′-diphosphate; $P2Y_1R$, purinergic receptor $P2Y_1$; PSD, postsynaptic density; TBST, Tris-buffered saline with Triton X-100.

References

Amadio, S., Tramini, G., Martorana, A., Viscomi, M.T., Sancesario, G., Bernardi, G. & Volonte, C. (2006) Oligodendrocytes express $P2Y_{12}$ metabotropic receptor in adult rat brain. *Neuroscience*, **141**, 1171–1180.

Anderson, M.F., Blomstrand, F., Blomstrand, C., Eriksson, P.S. & Nilsson, M. (2003) Astrocytes and stroke: networking for survival? *Neurochem. Res.*, **28**, 293–305.

Bachevalier, J. & Meunier, M. (1996) Cerebral ischemia: are the memory deficits associated with hippocampal cell loss? *Hippocampus*, **6**, 553–560.

Benvensiste, H., Drejer, J., Schousboe, A. & Diemer, N.H. (1984) Elevation of the extracellular concentrations of glutamate and aspartate in rat hippocampus during transient cerebral ischemia monitored by intracerebral microdialysis. *J. Neurochem.*, **43**, 1369–1374.

Bergersen, L.H., Magistretti, P.J. & Pellerin, L. (2005) Selective postsynaptic co-localization of MCT2 with AMPA Receptor GluR2/3 subunits at excitatory synapses exhibiting AMPA receptor trafficking. *Cereb. Cortex*, **15**, 361–370.

Bergersen, L., Ruiz, A., Bjaalie, J.G., Kullmann, D.M. & Gundersen, V. (2003) GABA and GABAa receptors at hippocampal mossy fibre synapses. *Eur. J. Neurosci.*, **18**, 931–941.

Bezzi, P., Gundersen, V., Galbete, J.L., Seifert, G., Steinhauser, C., Pilati, E. & Volterra, A. (2004) Astrocytes contain a vesicular compartment that is competent for regulated exocytosis of glutamate. *Nature Neurosci.*, **7**, 613–620.

Blum, D., Gall, D., Galas, M.C., d'Alcantara, P., Bantubungi, K. & Schiffmann, N.S. (2002) The adenosine A1 receptor agonist adenosine amine congener exerts a neuroprotective effect against the development of striatal lesions and motor impairments in the 3-nitropropionic acid model of neurotoxicity. *J. Neurosci.*, **22**, 9122–9133.

Braun, N., Zhu, Y., Krieglstein, J., Culmsee, C. & Zimmermann, H. (1998) Upregulation of the enzyme chain hydrolyzing extracellular ATP after transient forebrain ischemia in the rat. *J. Neurosci.*, **18**, 4891–4900.

Burnstock, G. (2004) Introduction: P2 receptors. *Curr. Top. Med. Chem.*, **4**, 793–803.

Chaudhry, F.A., Lehre, K.P., Van Lookeren Campagne, M., Ottersen, O.P., Danbolt, N.C. & Storm-Mathisen, J. (1995) Glutamate transporters in glial plasma membranes: highly differentiated localizations revealed by quantitative ultrastructural immunocytochemistry. *Neuron*, **14**, 711–720.

Choi, D.W. & Rothman, S.M. (1990) The role of glutamate neurotoxicity in hypoxic-ischemic neuronal death. *Annu. Rev. Neurosci.*, **13**, 171–182.

Ciruela, F., Casado, V., Mallol, J., Canela, E.I., Lluis, C. & Franco, R. (1995) Immunological identification of A1 adenosine receptors in brain cortex. *J. Neurosci. Res.*, **42**, 818–828.

Ciruela, F., Casado, V., Rodrigues, R.J., Lujan, R., Burgueno, J., Canals, M., Borycz, J., Rebola, N., Goldberg, S.R., Mallol, J., Cortes, A., Canela, E.I., Lopez-Gimenez, J.F., Milligan, G., Lluis, C., Cunha, R.A., Ferre, S. & Franco, R. (2006) Presynaptic control of striatal glutamatergic neurotransmission by adenosine A1–A2A receptor heteromers. *J. Neurosci.*, **26**, 2080–2087.

Cordeaux, Y., Ijzerman, A.P. & Hill, J.S. (2004) Coupling of the human A1 adenosine receptor to different heterotrimeric G proteins: evidence for agonist-specific G protein activation. *Br. J. Pharmacol.*, **143**, 705–714.

Cotman, C.W., Monaghan, D.T., Ottersen, O.P. & Storm-Mathisen, J. (1987) Anatomical organization of excitatory amino acid receptors and their pathways. *TINS*, **10**, 273–280.

Cunha, R.A., Johansson, B., Constantino, M.D., Sebastifio, A.M. & Fredholm, B.B. (1996) Evidence for high-affinity binding sites for the adenosine A2A receptor agonist [3H]CGS 21680 in the rat hippocampus and cerebral cortex that are different from striatal A2A receptors. *Naunyn-Schmiedeberg's Arch. Pharmacol.*, **353**, 261–271.

Dixon, C.J., Hall, J.F., Webb, T.E. & Boarder, M.R. (2004) Regulation of rat hepatocyte function by P2Y receptors: focus on control of glycogen phosphorylase and cyclic AMP by 2-methylthioadenosine 5′-diphosphate. *J. Pharmacol. Exp. Ther.*, **311**, 334–341.

Duarte, J.M.N., Oliveira, C.R., Ambrosio, A.F. & Cunha, R.A. (2006) Modification of adenosine A1 and A2A receptor density in the hippocampus of streptozotocin-induced diabetic rats. *Neurochem. Int.*, **48**, 144–150.

Dunwiddie, T.V. & Masino, S.A. (2001) The role and the regulation of adenosine in the central nervous system. *Annu. Rev. Neurosci.*, **24**, 31–55.

Franke, H., Grummich, B., Hartig, W., Grosche, J., Regenthal, R., Edwards, R.H., Illes, P. & Krugel, U. (2006a) Changes in purinergic signal after injury-involvement of glutamatergic mechanisms? *Int. J. Dev. Neurosci.*, **24**, 123–132.

Franke, H. & Illes, P. (2006) Involvement of P2 receptors in the growth and survival of neurons in the CNS. *Pharmacol. Ther.*, **109**, 297–324.

Franke, H., Krugel, U., Grosche, J., Heine, C., Hartig, W., Allgaier, C. & Illes, P. (2004) P2Y receptor expression onastrocytes in the nucleus accubens of rats. *Neuroscience*, **127**, 431–441.

Franke, H., Krügel, U. & Illes, P. (2006b) P2 receptors and neuronal injury. *Pflugers Arch.*, **452**, 622–644.

Franke, H., Krugel, U., Schmidt, R., Grosche, J., Reichenbach, A. & Illes, P. (2001) P2 receptor-types involved in astrogliosis *in vivo*. *Br. J. Pharmacol.*, **134**, 1180–1189.

Fredholm, B.B. (1997) Adenosine and neuroprotection. *Int. Rev. Neurobiol.*, **40**, 259–280.

Fredholm, B.B., Abbracchio, M.P., Burnstock, G., Daily, J.W., Harden, T.K., Jacobson, K.A., Leff, P. & Williams, M. (1994) Nomenclature and classification of purinoreceptors. *Pharmacol. Rev.*, **46**, 143–156.

Fredholm, B.B., Assender, J.W., Irenius, E., Kodama, N. & Saito, N. (2003) Synergistic effects of adenosine A_1 and P2Y receptor stimulation on calcium mobilization and PKC translocation in DDT1 MF-2 cells. *Cell. Mol. Neurobiol.*, **23**, 379–400.

Fumagalli, M., Trincavelli, L., Lecca, D., Martini, C., Ciana, P. & Abbracchio, M.P. (2004) Cloning, pharmacological characterisation and distribution of the rat G protein-coupled P2Y13 receptor. *Biochem. Pharmacol.*, **68**, 113–124.

Gao, Z.G., Blaustein, J.B., Gross, A.S., Melman, N. & Jacobson, K.A. (2003) N6-Substituted adenosine derivatives: selectivity, efficacy, and species differences at A3 adenosine receptors. *Biochem. Pharmacol.*, **65**, 1675–1684.

Giuntini, J., Giusti, L., Lucacchini, A. & Mazzoni, M.R. (2004) Modulation of A1 adenosine receptor signaling by peroxynitrite. *Biochem. Pharmacol.*, **67**, 375–383.

Gottlieb, M. & Matute, C. (1997) Expression of ionotropic receptor subunits in glial cells of the hippocampal CA1 area following transient forebrain ischemia. *J. Cereb. Blood Flow Metab.*, **17**, 290–300.

Gundersen, H.J., Bendtsen, T.F., Korbo, L., Marcussen, N., Moller, A., Nielsen, K., Nyengaard, J.R., Pakkenberg, B., Sorensen, F.B. & Vesterby, A. (1988) Some new, simple and efficient stereological methods and their use in pathological research and diagnosis. *APMIS*, **96**, 379–394.

Gundersen, V., Chaudhry, F.A., Bjaalie, J.G., Fonnum, F., Ottersen, O.P. & Storm-Mathisen, J. (1998) Synaptic vesicular localization and exocytosis of 1-aspartate in excitatory nerve terminals: a quantitative immunogold analysis in rat hippocampus. *J. Neurosci.*, **18**, 6059–6070.

Gylterud Owe, S., Bogen, I.L., Walaas, S.I., Storm-Mathisen, J. & Bergersen, L.H. (2005) Ultrastructural quantification of glutamate receptors at excitatory synapses in hippocampus of synapsin I+II double knock-out mice. *Neuroscience*, **136**, 769–777.

Hagberg, H., Lehmann, A. & Sandberg, M. (1985) Ischemia-induced shift of inhibitory and excitatory amino acids from intra- to extracellular compartments. *J. Cereb. Blood Flow Metab.*, **5**, 413–419.

Harry, G.J. & Lefebvre d'Hellencourt, C. (2003) Dentate gyrus: alterations that occur with hippocampal injury. *Neurotoxicology*, **24**, 343–356.

Hoffmann, C., Moro, S., Nicholas, R.A., Harden, T.K. & Jacobson, K.A. (1999) The role of amino acids in extracellular loops of the human P2Y1 receptor in surface expression and activation processes. *J. Biol. Chem.*, **274**, 14639–14647.

Hollopeter, G., Jantzen, H.M., Vincent, D., Li, G., England, L., Ramakrishnan, V., Yang, R.B., Nurden, P., Nurden, A., Julius, D. & Conley, P.B. (2001) Identification of the platelet ADP receptor targeted by antithrombotic drugs. *Nature*, **409**, 202–207.

Hourani, S.M.O., Bailey, S.J., Nicholls, J. & Kitchen, I. (1991) Direct effect of adenylyl 5′-(β-γ-methylene) diphosphonate, a stable ATP analogue, on relaxant P_1-purinoceptors in smooth muscle. *Br. J. Pharmacol.*, **104**, 685–690.

Jimenez, A.I., Castro, E., Communi, D., Boeynaems, J.M., Delicato, E.G. & Miras-Portugal, M.T. (2000) Coexpression of several types of metabotropic nucleotide receptors in single cerebellar astrocytes. *J. Neurochem.*, **75**, 2071–2079.

Jourdain, P., Bergersen, L.H., Bhaukaurally, K., Bezzi, P., Santello, M., Domercq, M., Matute, C., Tonello, F., Gundersen, V. & Volterra, V. (2007) Glutamate exocytosis from astrocytes controls synaptic strength. *Nature Neurosci.*, **10**, 331–339.

Kawamura, M., Gachet, C., Inoue, K. & Kato, F. (2004) Direct excitation of inhibitory interneurons by extracellular ATP mediated by P2Y1 receptors in the hippocampal slice. *J. Neurosci.*, **24**, 10835–10845.

Koizumi, S., Fujishita, K., Tsuda, M., Shigemoto-Mogami, Y. & Inoue, K. (2003) Dynamic inhibition of excitatory synaptic transmission by astrocyte derived ATP in hippocampal cultures. *Proc. Natl Acad. Sci. USA*, **100**, 11023–11028.

Lasley, R.D., Narayan, P., Uittenbogaard, A. & Smart, E.J. (2000) Activated cardiac adenosine A1 receptors translocate out of caveolae. *J. Biol. Chem.*, **275**, 4417–4421.

Lopes, L.V., Rebola, N., Pinheiro, P.C., Richardson, P.J., Oliveira, C.R. & Cunha, R.A. (2003) Adenosine A3 receptors are located in neurons of the rat hippocampus. *Neuroreport*, **14**, 1645–1648.

Lorenzen, A., Fuss, M., Vogt, H. & Schwabe, U. (1993) Measurement of guanine nucleotide-binding protein activation by A1 adenosine receptor agonists in bovine brain membranes: stimulation of guanosine-5′-*O*-(3-[^{35}S-thio) -triphosphate binding. *Mol. Pharmacol.*, **44**, 115–123.

Lorenzen, A., Guerra, L., Vogt, H. & Schwabe, U. (1996) Interaction of full and partial agonists of the A1 adenosine receptor with receptor/G protein complexes in rat brain membranes. *Mol. Pharmacol.*, **49**, 915–926.

Maemoto, T., Finlayson, K., Olverman, H.J., Akahane, A., Horton, R.W. & Butcher, S.P. (1997) Species differences in brain adenosine A1 receptor pharmacology revealed by use of xanthine and pyrazolopyridine based antagonists. *Br. J. Pharmacol.*, **122**, 1202–1208.

Masino, S.A., Diao, L., Illes, P., Zahniser, N.R., Larson, G.A., Johansson, B., Fredholm, B.B. & Dunwiddie, T.V. (2002) Modulation of hippocampal glutamatergic transmission by ATP is dependent on adenosine A_1 receptors. *J. Pharmacol. Exp. Ther.*, **303**, 356–363.

Mendoza-Fernandez, V., Andrew, R.D. & Barajas-Lopez, C. (2000) ATP inhibits glutamate synaptic release by acting at P2Y receptors in pyramidal neurons of hippocampal slices. *J. Pharmacol. Exp. Ther.*, **293**, 172–179.

Moore, D.J., Chambers, J.K., Murdock, P.R. & Emson, P.C. (2002) Human Ntera-2/D1 neuronal progenitor cells endogenously express a functional P2Y1 receptor. *Neuropharmacol.*, **43**, 966–978.

Moore, D., Chambers, J., Waldvogel, H., Faull, R. & Emson. P. (2000) Regional and cellular distribution of the P2Y1 purinergic receptor in the human brain: striking neuronal localization. *J. Comp. Neurol.*, **421**, 374–384.

Moran-Jimenez, M.J. & Matute, C. (2000) Immunohistochemical localization of the P2Y1 purinergic receptor in neurons and glial cells of the central nervous system. *Mol. Brain Res.*, **78**, 50–58.

Moro, S., Guo, D., Camaioni, E., Boyer, J.L., Harden, T.K. & Jacobson, K.A. (1998) Human P2Y1 receptor: molecular modeling and site-directed mutagenesis as tools to identify agonist and antagonist recognition sites. *J. Med. Chem.*, **41**, 1456–1466.

Munshi, R., Pang, I.H., Sternweis, P.C. & Linden, J. (1991) A1 adenosine receptors of bovine brain couple to guanine nucleotide-binding proteins G1, G2, and G0. *J. Biol. Chem.*, **286**, 22285–22289.

Murphy, K.M.M. & Snyder, S.H. (1982) Heterogeity of adenosine A1 receptor binding in brain tissue. *Mol. Pharmacol.*, **22**, 250–257.

Nagelhus, E.A., Veruki, M.L., Torp, R., Haug, F.M., Laake, J.H., Nielsen, S., Agre, P. & Ottersen, O.P. (1998) Aquaporin-4 water channel protein in the rat retina and optic nerve: polarized expression in Muller cells and fibrous astrocytes. *J. Neurosci.*, **18**, 2506–2519.

Nakata, H., Yoshioka, K. & Kamiya, T. (2004) Purinergic-receptor oligomerization: implications for neural functions in the central nervous system. *Neurotox. Res.*, **6**, 291–297.

Neary, J.T., Kang, Y., Willoughby, K.A. & Ellis, E.F. (2003) Activation of extracellular signal-regulated kinase by stretch-induced injury in astrocytes involves extracellular ATP and P2 purinergic receptors. *J. Neurosci.*, **23**, 2348–2356.

Newman, E.A. (2003) New roles for astrocytes: regulation of synaptic transmission. *TINS*, **26**, 536–542.

Niebauer, R.T., Gao, Z.G., Li, B., Wess, J. & Jacobson, K.A. (2005) Signaling of the human P2Y (1) receptor measured by a yeast growth assay with comparisons to assays of phospholipase C and calcium mobilization in 1321N1 human astrocytoma cells. *Purinergic Signal.*, **1**, 241–247.

Ochiishi, T., Chen, L., Yukawa, A., Saitoh, Y., Sekino, Y., Arai, T., Nakata, H. & Miyamoto, H. (1999) Cellular localization of adenosine A1 receptors in rat forebrain: immunohistochemical analysis using adenosine A1 receptor-specific monoclonal antibody. *J. Comp. Neurol.*, **411**, 301–316.

Ottersen, O.P., Zhang, N. & Walberg, F. (1992) Metabolic compartmentation of glutamate and glutamine: morphological evidence obtained by quantitative immunocytochemistry in rat cerebellum. *Neuroscience*, **46**, 519–534.

Palmer, R.K., Boyer, J.L., Schachter, J.B., Nicholas, R.A. & Harden, T.K. (1998) Agonist action of adenosine triphosphates at the human P2Y1 receptor. *Mol. Pharmacol.*, **54**, 1118–1123.

Piper, A.S. & Hollingsworth, M. (1996) ATP and β-γ-methylene ATP produce relaxation of guinea-pig isolated trachealis muscle via actions at P1 purinoceptors. *Eur. J. Pharmacol.*, **307**, 183–189.

Ponzio, T.A. & Hatton, G.I. (2005) Adenosine postsynaptically modulates supraoptic neuronal excitability. *J. Neurophysiol.*, **93**, 535–547.

Rathbone, M.P., Middlemiss, P.J., Gysbers, J.W., Andrew, C., Herman, M.A., Reed, J.K., Ciccarelli, R., Di Iorio, P. & Caciagli, F. (1999) Trophic effects of purines in neurons and glial cells. *Prog. Neurobiol.*, **59**, 663–690.

Rebola, N., Pinheiro, P.C., Oliveira, C.R., Malva, J.O. & Cunha, R.A. (2003) Subcellular localization of adenosine A_1 receptors in nerve terminals and synapses of the rat hippocampus. *Brain Res.*, **987**, 49–58.

Rebola, N., Rodrigues, R.J., Lopes, L.V., Richardson, P.J., Oliveira, C.R. & Cunha, R.A. (2005) Adenosine A1 and A2A receptors are co-expressed in pyramidal neurons and co-localized in glutamatergic nerve terminals of the rat hippocampus. *Neuroscience*, **133**, 79–83.

Rodrigues, R.J., Almeida, T., Richardson, P.J., Oliviera, C.R. & Cunha, R.A. (2005) Dual presynaptic control by ATP of glutamate release via facilitatory P2X1, P2X2/3, and P2X3 and inhibitory P2Y1, P2Y2, and/or P2Y4 receptors in the rat hippocampus. *J. Neurosci.*, **25**, 6286–6295.

Rudolphi, K.A., Schubert, P., Parkinson, F.E. & Fredholm, B.B. (1992) Adenosine and brain ischemia. *Cerebrovasc. Brain Metab. Rev.*, **4**, 346–369.

Sasaki, Y., Hoshi, M., Akazawa, C., Nakamura, Y., Tsuzuki, H., Inoue, K. & Kohsaka, S. (2003) Selective expression of Gi/o-coupled ATP receptor P2Y12 in microglia in rat brain. *Glia*, **44**, 242–250.

Swanson, T.H., Drazba, J.A. & Rivkees, S.A. (1995) Adenosine A1 receptors are located predominantly on axons in the rat hippocampal formation. *J. Comp. Neurol.*, **363**, 517–531.

Trincavelli, M.L., Marroni, M., Tuscano, D., Ceruti, S., Mazzola, M., Mitro, N., Abbracchio, M.P. & Martini, C. (2004) Regulation of A2B adenosine receptor functioning by tumor necrosis factor a in human astroglial cells. *J. Neurochem.*, **91**, 1180–1190.

Vohringer, C., Schafer, R. & Reiser, G. (2000) A chimeric rat brain P2Y1 receptor tagged with green-fluorescent protein: high-affinity ligand recognition of adenosine diphosphates and triphosphates and selectivity identical to that of the wild-type receptor. *Biochem. Pharmacol.*, **59**, 791–800.

Volonté, C., Amadio, S., D'Ambrosi, N., Colpi, M. & Burnstock, G. (2006) P2 receptor web: Complexity and fine-tuning. *Pharmacol. Ther.*, **112**, 264–280.

Von Kugelgen, I. (2006) Pharmacological profiles of cloned mammalian P2Y-receptor subtypes. *Pharmacol. Ther.*, **110**, 415–432.

Waldo, G.L. & Harden, T.K. (2004) Agonist binding and Gq-stimulating activities of the purified human P2Y1 receptor. *Mol. Pharmacol.*, **65**, 426–436.

Wang, L., Karlsson, L., Moses, S., Hultgardh-Nilsson, A., Andersson, M., Borna, C., Gudbjartsson, T., Jern, S. & Erlinge, D. (2002) P2 receptor expression profiles in human vascular smooth muscle and endothelial cells. *J. Cardiovasc. Pharmacol.*, **40**, 841–853.

Wang, B.L. & Larsson, L.I. (1985) Simultaneous demonstration of multiple antigens by indirect immunofluorescence or immunogold staining. Novel light and electron microscopical double and triple staining method employing primary antibodies from the same species. *Histochemistry*, **83**, 47–56.

Wardas, J. (2002) Neuroprotective role of adenosine in the CNS. *Pol. J. Pharmacol.*, **54**, 313–326.

Yoshioka, K., Hosoda, R., Kuroda, Y. & Nakata, H. (2002) Hetero-oligomerization of adenosine A1 receptors with P2Y1 receptors in rat brains. *FEBS Lett.*, **531**, 299–303.

Yoshioka, K. & Nakata, H. (2004) ATP- and adenosine-mediated signaling in the central nervous system: purinergic receptor complex: generating adenine nucleotide-sensitive adenosine receptors. *J. Pharmacol. Sci.*, **94**, 88–94.

Yoshioka, K., Saitoh, O. & Nakata, H. (2001) Heteromeric association creates a P2Y-like adenosine receptor. *Proc. Natl Acad. Sci. USA*, **98**, 7617–7622.

Zhang, F.L., Luo, L., Gustafson, E., Palmer, K., Qiao, X., Fan, X., Yang, S., Laz, T.M., Bayne, M. & Monsma, F. Jr (2002) $P2Y_{13}$: identification and characterization of a novel Galphai-coupled ADP receptor from human and mouse. *J. Pharmacol. Exp. Ther.*, **301**, 705–713.

Zhu, Y. & Kimelberg, H.K. (2001) Developmental expression of metabotropic P2Y1 and P2Y2 receptors in freshly isolated astrocytes from rat hippocampus. *J. Neurochem.*, **77**, 530–541.

Zimmermann, H. (2000) Extracellular metabolism of ATP and other nucleotides. *Naunyn Schmiedebergs Arch. Pharmacol.*, **362**, 299–309.